INTERNATIONAL JOURNAL OF COMMUNICATION SYSTEMS
Int. J. Commun. Syst. (2010)
Published online in Wiley Online Library (wileyonlinelibrary.com). DOI: 10.1002/dac.1167

Performance improvement of fixed wireless access networks by conjunction of dual polarization and time domain radio resource allocation technique‡

Alexander Vavoulas*,†, Nicholas Vaiopoulos, Dimitris A. Varoutas, Aris Chipouras and George Stefanou

Department of Informatics and Telecommunications, University of Athens, Athens, Greece

SUMMARY

This paper considers the impact of dual polarization adoption on the performance for a fixed wireless access (FWA) network. The major limiting factor of the performance in these systems is co-channel interference (CCI) originating from intracell and intercell concurrent transmissions. The proposed framework combines an appropriate time domain radio resource allocation technique with a dual polarization pattern to mitigate CCI and enhance the obtained signal to interference plus noise ratio (SINR). Simulation results present the performance of the proposed framework against various terrain categories and sector antenna characteristics.

Received 30 September 2009; Revised 10 March 2010; Accepted 24 May 2010

KEY WORDS: wireless communications; co-channel interference; polarization allocation; radio resource management

1. INTRODUCTION

The vision of 'broadband to all' has necessitated the deployment of fixed wireless access (FWA) as an alternative technology in order to provide broadband access to geographical areas where the cost of wired infrastructure is extremely high. For a long time, the development of FWA systems was strongly related to the requirement of line of sight (LOS) condition. However, the development of the IEEE 802.16 WirelessMAN standard [1] induced an increasing interest for systems providing wireless broadband services under non-line of sight (NLOS) conditions in the 2–11 GHz frequency range. On the other hand, the continuously growing demand for higher data rates and bandwidth-consuming services becomes a driving force toward larger channel widths and wider spectrum block allocation consequently. Traditional frequency planning with high reuse patterns wastes the limited available spectrum, especially in the lower regions of the 2–11 GHz band, and a full frequency reuse in each sector of each cell is a very attractive alternative to fulfill

*Correspondence to: Alexander Vavoulas, Department of Informatics and Telecommunications, University of Athens, Athens, Greece.
†E-mail: vavoulas@di.uoa.gr
‡This paper was presented in part at the 18th IEEE PIMRC, Athens, Greece, September 2007.

this challenge. However, such an approach results in high co-channel interference (CCI), which arises from concurrent intracell and intercell transmissions, and affects significantly the users' quality of service (QoS).

Several approaches have been proposed in the literature for CCI reduction. An increased effort is focused on the corresponding time domain radio resource allocation techniques (RRA) [2–4] in order to organize the total amount of interference. Additionally, the use of alternate polarization allocation (PA), as a mean to decrease the interference into the desired signal, is introduced in systems operating under LOS conditions [5]. Specifically, in [2] a heuristic scheduling mechanism along with a terminal classification procedure has been proposed for interference reduction. This concept is improved with the different scheduling mechanisms for odd and even sectors [3]. In [4], the scheme is extended with the introduction of power shaping concept. On the other hand, an alternate PA scheme for local multipoint distribution service (LMDS) operating under LOS conditions is presented in [6]. A PA scheme for systems under NLOS operation is proposed in [7] so as to further assist the channel allocation policy and reduce the CCI.

Hence, it would be interesting to investigate a possible system performance enhancement, for an FWA system operating under NLOS conditions, by jointly utilizing a time domain RRA technique and an alternate PA scheme.

The remainder of the paper is organized as follows. In Section 2, a brief introduction of the system under investigation is given whereas the details of the proposed framework and the performance of downlink are described in Sections 3 and 4, respectively. In Section 5, simulation results are given for a practical FWA network concerning the throughput performance. Eventually, concluding remarks are given in Section 6.

2. FWA CELLULAR ARCHITECTURE

In this paper, the downlink of a time division multiple access (TDMA) fixed cellular network is examined based on single carrier technology and designed for NLOS operation. Time domain scheduling with S terminals per sector and full frequency reuse in the 2–11 GHz frequency bands are assumed. The service area is divided into hexagonal cells and triangular sectors [2, 3]. Each sector is equipped with its own directional antenna and is labelled from 1 to 6 counter-clockwise, in such a way that there are no adjacent sectors bearing the same label (Figure 1). The labels of three adjacent cells are rotated by 120°, in respect to one another, creating a cluster (contained in the heavy line in Figure 1) whose pattern is repeated across the entire service area. Adjacent sector antennas use orthogonal polarization so as to maximize isolation among them and increase the communication quality. Users use rooftop directional antennas pointing to their respective sector antenna following the polarization pattern. The beamwidth of a sector antenna has to be wide enough in order to serve the entire sector, whereas the beamwidth of each terminal antenna must be more directional to lower interference.

3. IMPACT OF PA ON CCI REDUCTION

3.1. Propagation modelling

Although many propagation models have been proposed in the literature for mobile networks, the determination of an appropriate propagation model for FWA networks is still an open issue.

DOI: 10.1002/dac

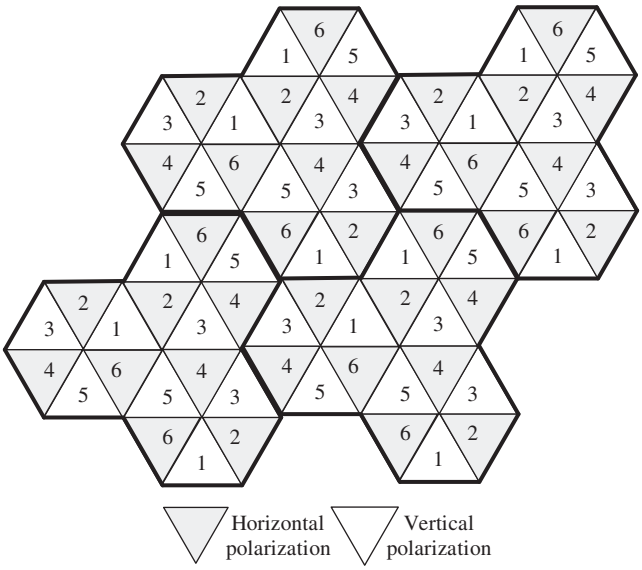

Figure 1. A representative part of the hexagonal cell layout consisting of four clusters.

A well-known propagation model [8] is adopted for the system under examination, which includes the distance-dependent path loss, the lognormal shadowing, from trees and structures, as well as the cross polarization discrimination (XPD) between transmitter and receiver antennas. The effect of multipath delay spread in the reception is minor because of the adopting of high directional sector and terminal antennas [9] and is omitted in the link budget calculations. The effect of small-scale fading is negligible since the sector and terminal antennas are placed in fixed positions.

The value of XPD is a quantitative measure for signal depolarization and is defined as the ratio between the useful co-polar received signal and the interfering signal received in the cross-polar (orthogonal) polarization. The main sources for signal depolarization are foliage, tree density and precipitation. However, it has been shown that the depolarization due to precipitation is significantly reduced for carrier frequencies below 11 GHz [10] and the XPD is a very weak function of co-polarized attenuation. The adoption, therefore, of a constant XPD value is a reasonable simplified assumption for the link budget calculations [8].

The distance-dependent path loss is determined for three terrain categories according to [11]. More precisely, category A corresponds to the maximum path loss condition (hilly terrain with moderate to heavy tree densities), category C to the minimum one (mostly flat terrain with light tree densities) whereas category B captures the intermediate path loss condition. For a given close-in distance d_0, the path loss, PL, is given by

$$\mathrm{PL} = \left(\frac{\lambda}{4\pi d_0}\right)^2 \cdot \left(\frac{d_0}{d}\right)^{\gamma} \cdot s \tag{1}$$

where λ is the wavelength (in meters), d is the distance from the corresponding sector antenna and s is a random variable representing the lognormal shadowing with zero mean and σ dB standard deviation. Additionally, γ is the path loss exponent with $\gamma = \gamma_1 - \gamma_2 \cdot h_B + \gamma_3 / h_B$ (h_B is the sector

DOI: 10.1002/dac

antenna height, γ_1, γ_2, γ_3 are constants). The values of σ, γ_1, γ_2 and γ_3 depend on the terrain category given in [11].

The average power received at terminal j of sector l from the antenna of sector k is given by

$$P_j = P_t \cdot G_{jk} \cdot \left(\frac{\lambda}{4\pi d_0}\right)^2 \cdot \left(\frac{d_0}{d_{jk}}\right)^{\gamma} \cdot s_{jk} \cdot \begin{cases} \dfrac{1}{\text{XPD}} & \text{for cross-polarized sectors} \\ \dfrac{\text{XPD}-1}{\text{XPD}} & \text{for co-polarized sectors} \end{cases} \tag{2}$$

where P_t is the fixed transmitted power, G_{jk} is the composite transmit–receive antenna gain, and XPD is the value of cross polarization discrimination. The signal strength received at terminal j from serving sector antenna l is given for $k=l$.

3.2. CCI calculation

The CCI is calculated by taking into account the impact of intracell and intercell interference separately. The corresponding signal to interference plus noise ratios (SINRs), for each sector l, are given by the following equations:

$$\text{SINR}_{\text{intra}} = \frac{G_{jl}}{\sum_{k\neq l} \bmod_2(k+\delta)\cdot G_{jk} + \sum_k \bmod_2(k+\delta+1)\cdot \dfrac{G_{jk}}{\text{XPD}-1} + \dfrac{N}{\text{XPD}-1}} \tag{3}$$

$$\text{SINR}_{\text{inter}} = \frac{G_{jl}\cdot s_{jl}\cdot d_{jl}^{-\gamma}}{\sum_n \left(\sum_k \bmod_2(k+\delta)\cdot G_{jnk}\cdot s_{jn}\cdot d_{jn}^{-\gamma} + \sum_k \bmod_2(k+\delta+1)\cdot \dfrac{G_{jnk}\cdot s_{jn}\cdot d_{jn}^{-\gamma}}{\text{XPD}-1}\right) + \dfrac{N}{\text{XPD}-1}} \tag{4}$$

where n is the number of neighboring cells, k the number of sectors per cell, G_{jnk} the composite transmit–receive antenna gain from sector k of cell n, d_{jn} the distance from sector antennas of cell n and $\delta=0$ for odd sectors ($l=1, 3, 5$) and $\delta=1$ for even sectors ($l=2, 4, 6$).

Considering an FWA network without a PA pattern, it is clear that the most significant amount of intracell interference, for each sector, is originating from its two adjacent sectors due to the overlapping sector antenna patterns. However, under the proposed framework, each sector antenna is transmitting with orthogonal polarization with respect to its adjacent sector antennas. Hence, the amount of intracell interference is significantly reduced according to (3).

On the other hand without loss of generality, the impact of intercell interference is examined for sector 1 of the central cell as presented in Figure 1. Considering a cellular architecture without a PA pattern, it is clear that the most significant amount of intercell interference is originating from the across intercell sector antenna 3 (because of the front lobe of sector antenna 3 that points directly to the terminals of the tagged sector) and the opposite intercell sector antenna 2. However, it is shown from (4) that the proposed PA pattern reduces significantly the impact of intercell sector antenna 2 due to the transmission under orthogonal polarization with respect to the sector under examination. Finally, it is important to note that intercell interference is low compared with intracell interference due to the distance-dependent path loss as well as the high front to back (FTB) ratio of terminal antennas.

DOI: 10.1002/dac

4. FRAME STRUCTURE AND DOWNLINK PERFORMANCE

The CCI reduction is accomplished with an appropriate RRA technique adoption. The TDMA frame is always divided into $K=6$ subframes equal to the number of sectors per cell. Each sector schedules packets for transmissions, starting from A and following the staggered order A, B, C, D, E and F [3], shown in Figure 2. The purpose of this scheduling is to manage more efficiently the impact of major intracell and intercell interferers.

Each terminal is classified, for a given SINR threshold ($\mathrm{SINR_{thr}}$), through an iterative procedure found in [1–3] according to its SINR in its k-th subframe given by:

$$\mathrm{SINR}=((\mathrm{SINR_{intra}})^{-1}+(\mathrm{SINR_{inter}})^{-1})^{-1} \tag{5}$$

It must be noticed that an interference limited scenario is considered and the effect of thermal noise is negligible in the SINR calculations. Each subframe is further divided into six mini-frames allowing different degrees of concurrent transmissions in each subframe [2, 3]. The degree of concurrent transmissions of each mini-frame is denoted by its label (Figure 2). In other words, only class-i terminals are served in mini-frame i. Each sector can use mini-frame i in i different subframes.

The number of timeslots n_i of mini-frame i, $i\in\{1,..,6\}$, in each subframe is appropriately chosen to handle the uniform traffic load among terminals [2]. Therefore

$$n_i=\left[\frac{N_t\cdot\dfrac{a_i}{i}}{\sum_{j=1}^{6}\dfrac{a_j}{j}}\right] \tag{6}$$

where α_i is the fraction of class i terminals, N_t the total number of timeslots in each subframe and [x] the rounded x according to the Hamilton/Hare rounding procedure [4]. This procedure consists of two stages. In the first stage, the number of timeslots n_i is rounded down to their integer parts and in the second stage the remaining timeslots are assigned to mini-frames starting from the ones with the largest remainder fractional parts. The sum of the fractions α_i for all classes gives the total fraction of terminals that can be served and is mentioned as coverage C.

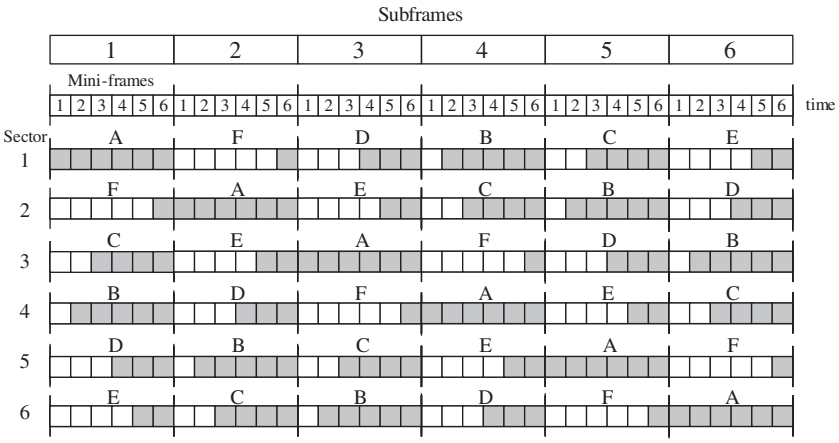

Figure 2. Order of subframe use and available miniframes according to [3].

DOI: 10.1002/dac

The maximum normalized downlink throughput per sector for the system under examination is finally approximated in [2] by:

$$\tau = \sum_i \tau_i = \sum_i \frac{i \cdot n_i}{K \cdot N_t} \quad \text{(packets/slot/sector)} \tag{7}$$

where τ_i is the maximum downlink throughput of each class.

5. SIMULATION RESULTS

Simulation results have been obtained in order to study the maximum throughput (packets/slot/sector) of the proposed framework (RAAMI-PA). The simulated fixed cellular networks includes 19 hexagonal cells. The examined sector is the one with the greatest amount of interference (that is the worst case scenario) placed into the middle cell and assumed that it serves $S = 1500$ terminals uniformly placed. The path loss model presented in Section 3 is adopted. The values of the path loss exponent and the standard deviation of shadowing, according to each terrain category, are given in Table I. The value of the sector antenna height h_B is taken to be equal to 80 m. Typical directional antenna patterns, compliant with the specifications in [12], are used for sector and terminal antennas. Unless specified otherwise, the FTB ratio and the 3 dB beamwidth of sector and terminal antennas are (25, 15) dB and (45°, 30°), respectively, and the value of the XPD is equal to 20 dB. The reference SINR_{thr} for successful packet transmission is taken to be equal to 15 dB, a value compliant with the provided QoS needed for the most of the services offered by an FWA network.

The impact of sector antenna parameters on maximum throughput per sector, following both frameworks, for the three terrain categories is shown in Figures 3 and 4. Specifically, in Figure 3 an obtained maximum throughput improvement up to 95% is evident, with respect to the 3 dB beamwidth of sector antenna. Obviously, the use of less directional antennas is possible with the adoption of RAAMI-PA. Indeed, the throughput is almost constant for the range 40°–70° of 3 dB beamwidth of sector antenna due to the exploitation of the transmission under orthogonal polarization of the dominant interferers. In both cases, the coverage is the same.

Similarly, Figure 4 shows the obtained maximum throughput improvement with respect to the FTB ratio of sector antenna. A noticeable maximum throughput improvement (almost

Table I. Path loss calculation parameters [11].

	Category		
Parameter	Terrain C (Flat few trees)	Terrain B (Intermediate)	Terrain A (Hilly heavy trees)
a	3.6	4.0	4.6
b	0.0050	0.0065	0.0075
c	20.0	17.1	12.6
Channel frequency f (GHz)	3.5	3.5	3.5
BS antenna height h_B (m)	80	80	80
Path loss exponent $\gamma = a - b \cdot h_B + c/h_B$	3.4500	3.6938	4.1575
Standard deviation of shadowing s (dB)	8.2	9.6	10.2
Reference distance d_0 (m)	100	100	100
$A = 20 \cdot \log_{10}(4 \cdot \pi \cdot d_0/\lambda)$	82.3231	82.3231	82.3231

DOI: 10.1002/dac

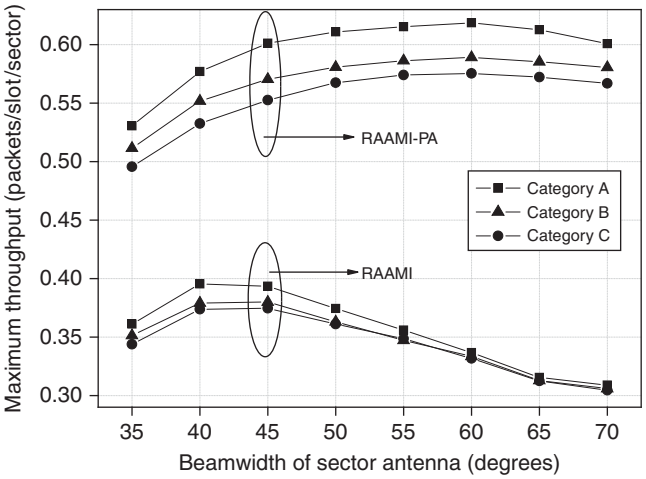

Figure 3. Maximum throughput per sector vs beamwidth of sector antenna. The FTB ratio of sector and terminal antennas are 25 and 15 dB, respectively whereas the 3 dB beamwidth of terminal antenna equals to 30° ($SINR_{thr} = 15\,dB, XPD = 20\,dB$).

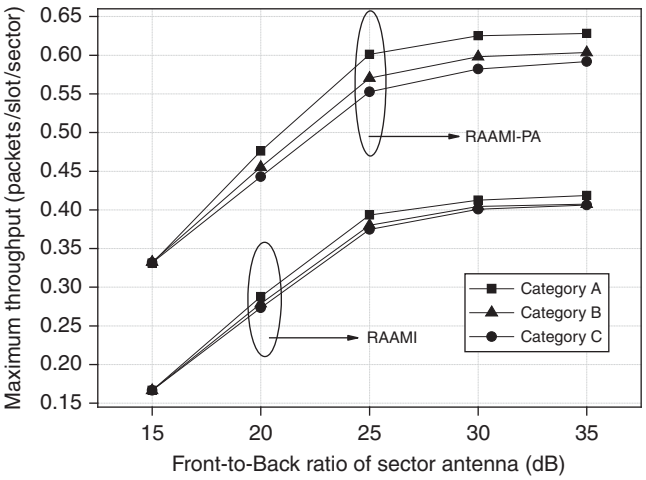

Figure 4. Maximum throughput per sector (a) and coverage (b) vs FTB of sector antenna. The 3 dB beamwidth of sector and terminal antennas are 45° and 30°, respectively, whereas the FTB ratio of terminal antenna equals to 15 dB ($SINR_{thr} = 15\,dB, XPD = 20\,dB$).

100%) is obtained under the proposed framework even when the FTB ratio of sector antenna is small.

The impact of XPD on the maximum throughput per sector for the three terrain categories under the proposed framework is presented in Figure 5. As expected when the value of the XPD is increasing, the maximum throughput per sector is increasing as well, since the orthogonal frequency reuse among adjacent sectors becomes more effective. However, it is noticed that above 20 dB the maximum throughput per sector remains substantially constant and the use of antennas with better XPD characteristics is proven meaningless.

DOI: 10.1002/dac

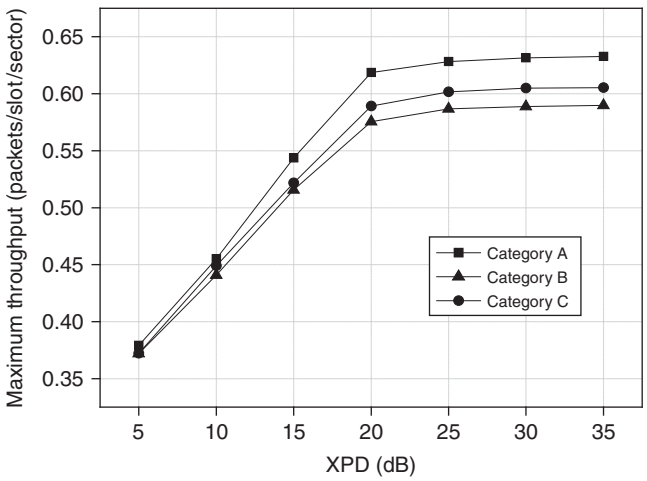

Figure 5. Maximum throughput per sector vs XPD. The 3 dB beamwidth of sector and terminal antennas are 45° and 30°, whereas the FTB ratio of sector and terminal antennas are 25 and 15 dB, respectively ($SINR_{thr} = 15$ dB).

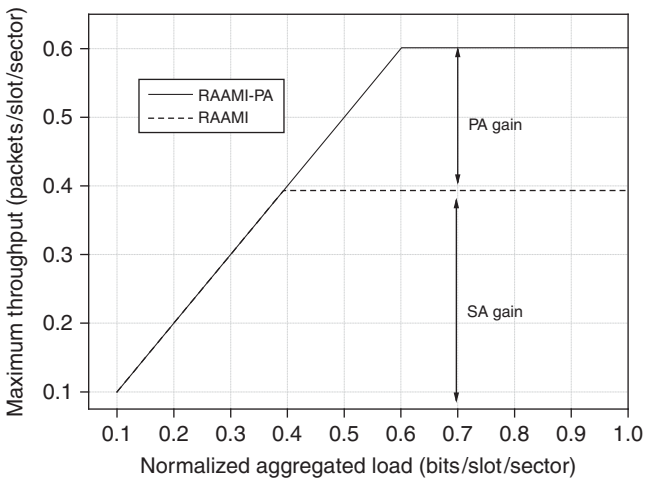

Figure 6. Maximum throughput per sector vs normalized aggregated load for terrain category B. The 3 dB beamwidth of sector and terminal antennas are 45° and 30°, whereas the FTB ratio of sector and terminal antennas are 25 and 15 dB, respectively ($SINR_{thr} = 15$ dB, XPD = 20 dB).

Finally, in Figure 6 the maximum throughputs of RAAMI and RAAMI-PA in terms of the normalized aggregated load are compared. In this case, a value of XPD equals to 20 dB and the terrain category B is considered. For a normalized aggregated load up to 0.4, both methods achieve the same maximum throughput. As the traffic increases more, it is clear that the adoption of the PA concept induces a maximum throughput per sector enhancement reaching about 50%. Consequently, the proposed framework consists of a serious candidate for the emerging wireless technologies like WiMAX.

DOI: 10.1002/dac

6. CONCLUSION

An integrated time domain RRA technique of concurrent transmissions and polarization alternation pattern is proposed and analyzed for the downlink direction of an FWA system. The proposed scheme outperforms the RAAMI RRA since the PA pattern incorporation reduces significantly the impact of dominant interferers. It is worth mentioning that the proposed scheme performs better under worst propagation conditions (terrain category A) and exploits better low-performance antennas, which present large beamwidths and small FTB ratios.

REFERENCES

1. Ghosh A, Wolter DR, Andrews JG, Chen R. Broadband wireless access with WiMax/802.16: current performance benchmark and future potential. *IEEE Communications Magazine* 2005; **43**:129–135.
2. Leung KK, Srivastava A. Dynamic allocation of downlink and uplink resource for broadband services in fixed wireless networks. *IEEE Journal on Selected Areas in Communications* 1999; **17**:990–1006.
3. Vaiopoulos N, Vavoulas A, Varoutas D, Sphicopoulos T. A radio resource allocation scheme for fixed broadband wireless access systems with avoidance of major interferers. *Wireless Personal Communications* 2007; **40**:479–487.
4. Tralli V, Veronesi R, Zorzi M. Power-shaped advanced resource assignment (PSARA) for fixed broadband wireless access systems. *IEEE Transactions on Wireless Communications* 2004; **3**:2207–2220.
5. Roman V. Frequency re-use and system deployment in Local Multipoint Distribution Service. *IEEE Personal Communications* 1999; **6**:20–27.
6. Panagopoulos AD, Arapoglou PDM, Kanellopoulos JD, Cottis PG. Intercell radio interference studies in broadband wireless access networks. *IEEE Transactions on Vehicular Technology* 2007; **56**:3–12.
7. Ntagkounakis K, Sharif B, Dallas P. Novel channel and polarization assignment schemes for 2–11 GHz fixed-broadband wireless access networks. *Wireless Personal Communications* 2006; **36**:425–443.
8. Farahvash S, Kavehrad M. Co-channel interference assessment for Line-of-Sight and Nearly Line-of-Sight millimeter-waves cellular LMDS architecture. *International Journal of Wireless Information Networks* 2000; **7**:197–210.
9. Erceg V, Greenstein LJ, Tjandra SY, Parkoff SR, Gupta A, Kulic B, Julius AA, Bianchi R. A model for the multipath delay profile of fixed wireless channels. *IEEE Journal on Selected Areas in Communications* 1999; **17**:399–410.
10. Fong B, Rapajic PB, Fong ACV, Hong GY. Polarization of received signals for wideband wireless communications in a heavy rainfall region. *IEEE Communications Letters* 2003; **7**:13–14.
11. IEEE. IEEE standard for local and metropolitan area networks, part 16: air interface for fixed broadband wireless access systems—amendment 2: medium access control modifications and additional physical layer specifications for 2–11 GHz, 2003.
12. ETSI. Fixed radio systems; point-to-multipoint antennas; antennas for point-to-multipoint fixed radio systems in the 3 GHz to 11 GHz band, 2005.

AUTHORS' BIOGRAPHIES

Alexander Vavoulas was born in Athens, Greece in July 1976. He received the BSc degree in Physics and the MSc degree in Electronics and Radio-Communications in 2000 and 2002 respectively, both from the University of Athens, Greece. He is currently working toward the PhD degree at the same University. Since 2009 he has been a Special and Laboratorial Teaching Staff in the Department of Computer Science and Biomedical Informatics at the University of Central Greece. His major research interests include physical and MAC layer issues for broadband wireless access systems and technoeconomic evaluation of network services. He is a student member of Communications and Vehicular Technology Societies of IEEE and serves as reviewer in several journals and conferences.

DOI: 10.1002/dac

Nicholas Vaiopoulos was born in Lamia, Greece in 1977. He received his Physics degree and his MSc degree in Electronics and Radio-Communications from the University of Athens, Greece in 2000 and 2003, respectively. Currently, he is working towards his PhD degree on the resource allocation techniques with reference to wireless systems in the Department of Informatics and Telecommunications at the same University. Since 2009 he is a Special and Laboratorial Teaching Staff in the Department of Computer Science and Biomedical Informatics at the University of Central Greece. His research interests include broadband communications systems, scheduling algorithms and power control techniques for wireless systems.

Dimitris Varoutas holds a Physics degree and MSc and PhD diplomas in Communications and Technoeconomics from the University of Athens. He is a lecturer in telecommunications technoeconomics in the Department of Informatics and Telecommunications at the University of Athens. He has been participating in numerous European R&D projects in the RACE I & II, ACTS, Telematics, RISI and IST frameworks in the areas of telecommunications and technoeconomics. He actively participates in several technoeconomic activities for telecommunications, networks and services such as the ICT–OMEGA and the CELTIC/CINEMA projects, as well as Conferences on Telecommunications TechnoEconomics. He also participates in or manages related national activities for technoeconomic evaluation of broadband strategies, telecommunications demand forecasting, price modelling etc. His research interests span design of optical and wireless communications systems to technoeconomic evaluation of network architectures and services. He has published more than 50 publications in refereed journals and conferences in the area of telecommunications, optoelectronics and technoeconomics, including leading IEEE Journals and conferences. He is a member of IEEE and serves as reviewer in several journals and conferences including IEEE.

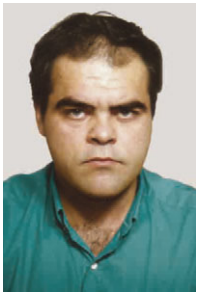

Aris Chipouras was born in Boston U.S.A. in 1962. He received the BSc degree in Physics, in 1985, the MSc degree in Electronics and Radio-Communications in 1987, the MSc degree in Information Systems in 1994, and the PhD in Informatics & Telecommunications in 2002, all from the University of Athens, Greece. Since 1993, he is a researcher associate with the Optical Communications Group, University of Athens, participating in several European R&D projects. His current research interests include the analysis and design of microwave integrated circuits, optical waveguide devices as well as the multi-wavelength optical networks and wireless communications systems. He has several publications in journals and conferences in the area of optical communications.

George Stefanou photograph and biography not available at the time of publication.

DOI: 10.1002/dac